NJC

Accepted Manuscript

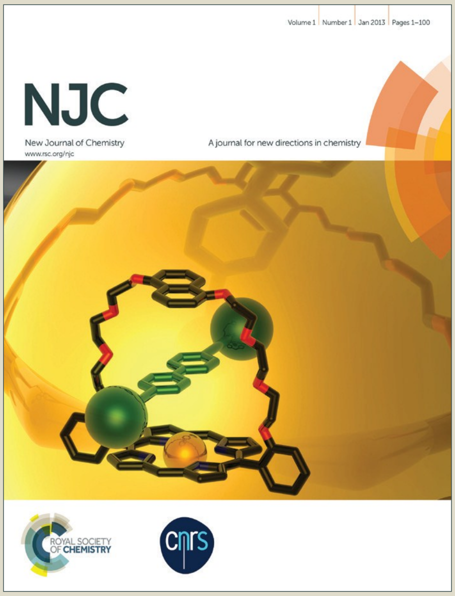

ROYAL SOCIETY OF CHEMISTRY

www.rsc.org/njc

New Journal of Chemistry Dynamic Article Links ►

Cite this: DOI: 10.1039/c0xx00000x

www.rsc.org/xxxxxx PAPER

Exploring excited state properties of 7-hydroxy and 7-methoxy 4-Methycoumarin: A combined time-dependent density functional theory / effective fragment potential study

Mariyappa Ramegowda,*[a] Keremegaladoddi N Ranjitha,[a] Thalashasana N Deepika[a]

Received (in XXX, XXX) Xth XXXXXXXXX 20XX, Accepted Xth XXXXXXXXX 20XX
DOI: 10.1039/b000000x

Effective fragment potential (EFP) method of solvation interfaced with the density functional theory (DFT) was applied to investigate the hydrogen bonding (HB) sites of 7-hydroxy-4-Methylcoumarin (4MU (4-Methylumbelliferone)) and 7-methoxy-4-Methylcoumarin (MMC) in water. The original EFP model (EFP1) is used to form 4MU-$(H_2O)_5$, $4MU^{-}$-$(H_2O)_5$, 4MUT-$(H_2O)_5$ (keto tautomer of 4MU) and MMC-$(H_2O)_2$ complexes. A hydrogen bond network is formed by three water molecules between oxygen of the carbonyl group and hydrogen (oxygen) of the hydroxyl group. Five HBs are formed by 4MU and 4MUT with water molecules; two C=O···H (B type), one C-O···H (B′ type), one by oxygen of the pyrone ring with hydrogen of hydroxyl group or water molecule (B′′ type) and one O-H···O (type C). $4MU^{-}$ also formed five HBs; two B type, two B′ type and one B′′ type. Two HBs are formed by MMC; one B type and one B′ type. Excited state properties are computed using state specific time dependent density functional theory (SS-TDDFT) combined with the polarizable continuum model (PCM) and EFP1 method. The excited state hydrogen transfer (ESHT) is found in the first excited (S_1) state of 4MU. C-OH bond contracting, O-H bond stretching and O-H···O HB strengthening suggests the possibility of hydrogen transfer from the hydroxyl group to water molecule and water molecule to the carbonyl group at S_1 state. The natural charge analysis manifests the intramolecular charge transfer (ICT) of 4MU chromophore in the S_1 state, and also the calculated electronic absorption and fluorescence spectra of 4MU, $4MU^{-}$ and 4MUT in water reveals the tendency of hydrogen transfer in the S_1 state. The change in HB energy between 4MU-$(H_2O)_5$ complex at the S_0 state and 4MUT-$(H_2O)_5$ complex at the S_1 state confirms the formation of 4MUT-$(H_2O)_5$ complex at the first excited state.

Introduction

A nonspecific interaction between solute and solvent molecules is the long-range interaction and is mainly due to the dielectric properties of the solvent, arising from Coulombic forces.[1] However, in addition to the Coulombic interaction, a solute molecule consisting of an atom or a group with a lone pair of electrons may form a hydrogen bonded complex with one of the solvent molecules having a proton-donating group.[2] The hydrogen bond interaction in both the ground and excited-states, play a fundamental role in the photochemistry of organic and biological chromophores in solution.[3] The intermolecular hydrogen bonds, including their structure and energy in both ground and excited states have been extensively studied theoretically[4] and experimentally.[5] A theoretical work by Zhao et al.[4d] demonstrated that the excited-state HB weakening can heighten the excitation energy of a related excited state and induce an electronic spectral blueshift, whereas the excited-state HB strengthening can lower the excitation energy of a related excited state and induce an electronic spectral redshift. Many molecules of donor-acceptor character, often used as probes, in their ground and excited electronic states can form hydrogen bonds with protic solvent molecules. Apart from the influence of the solvent polarity and polarizability, HBs formed between the probes and solvents also influence their structure and photophysical properties.[6] The formation of hydrogen bonds can often lead to the appearance of new individuals like S_0-complexes and S_1 exciplexes.[7]

The effective fragment potential[8a] is a discrete method that accounts for solvent molecules explicitly and provides a polarizable QM-based force field to describe intermolecular interactions. There are two EFP methods: EFP1 and EFP2 in which EFP1 method was developed specifically for water.[8] The EFP method embedded with PCM, have been applied successfully to QM/MM studies of molecules in clusters and in solution. Arora et al.[9] have interfaced configuration interaction with single excitations (CIS) with the EFP method for studying the qualitative effects of solvents on the electronic spectra of molecules. Minezawa et al.[10] implemented the analytic energy gradient for the combined TDDFT/EFP1 method to describe the excited state dynamics of solvated molecules. Yoo et al.[11] have combined the linear response TDDFT (LR-TDDFT) method with EFP1 model and applied the hybrid method successfully to simulate the absorption spectrum of the n→π* vertical transition of acetone in aqueous solution. The interface of the EFP1 model with the TDDFT method has been developed for describing electronically excited states of solvated molecules.

Proton coupled electron transfer (PCET) reactions, which occurs at ground state, play a major role in many systems of biological relevance, including, for instance, those responsible for nitrogen or oxygen fixation.[12] PCET reactions are extensively studied by various researchers experimentally and theoretically.[13] Recently several studies focused on the possibility of inducing proton transfer/ hydrogen atom transfer (PT/HT) under irradiation, giving rise to the so-called excited state proton transfer/ hydrogen atom transfer (ESPT/ESHT) reactions.[14] The irradiation produces the ICT excited state allowing for its deprotonation/ dehydrogenation from the protonated/hydrogenated site of the molecule. The consequent PT/HT reaction can occur either at the intra or intermolecular level (for instance, to a solvent molecule).

Coumarins present a variety of bioactivities, including anticoagulant, estrogenic, dermal photosensitizing, antimicrobial, vasodilator, molluscicidal, antihelmintic, sedative and hypnotic, analgesic and hypothermic actions.[15] Coumarin derivatives exhibit not only excellent biological and medical activities, but also have superior thermal stability and outstanding optical properties, including extended spectral responses, high quantum yields, and superior photostability. Optical applications of these compounds, such as laser dyes, nonlinear optical chromophore, fluorescent whiteners, fluorescent probes, optical recording and solar energy collectors, have been widely investigated.[16]

Hydroxy coumarins, such as 4MU, are the fluorescent molecules with UV/UV-Vis excitation wavelengths, finding applications in diverse fields.[17] They can be used as laser dyes, colorants, chromophores or fluorophores.[18] Also, they have been widely investigated for their biological activity as antifungals,[19] anticarcinogens,[20] enzyme inhibitors,[21] and spasmolytic and sun-screening additives.[22] M. Savarese et al.[23] correlate the charge transfer character of ESPT to the main photophysical features of the reaction of 7- hydroxy-4-(trifluoromethyl)coumarin.

The spectral properties and HB dynamics of aminocoumarin derivatives have been studied extensively by number of researchers[3a,b,i,j,l,4a-c,j,k] and shows that the decrease in A type (N···H) HB energy for the S_1 state relative to the S_0 state was much smaller than the increase in energy of B and C type HBs formed by the carbonyl group and N-H bond, respectively. Zhao et al.[3k] affirmed that, in addition to solvent polarity, HBs formed between Coumarin 120 and solvent molecules also significantly affect its electronic transition energies. According to these references, formation of A type HB causes blueshift in the absorption maximum, whereas formation of B and C type HBs results in redshift. The results of many calculations indicate that, in the excited states of hydrogen-bonded coumarin-solvent complexes, B and C type HBs are stronger, whereas A type HB is weaker.[3h-l,4a-c] These results are consistent with the earlier observed blueshift of the long wavelength band of the absorption spectra of coumarin derivatives in water.[5f,6,7a] The excited-state hydrogen bonding dynamics of aminocoumarin derivatives in water have been studied[4a-c,7a] and demonstrated that A type HB is the strongest hydrogen bond among three ones in the S_0 state and it is extremely weakened in S_1 state, which is significantly greater than the strengthening of B and C type HBs. Taking into regard the complex character of HBs made by aminocoumarin molecules, it is important to study these hydrogen-bond interactions in both S_0 and S_1 states.

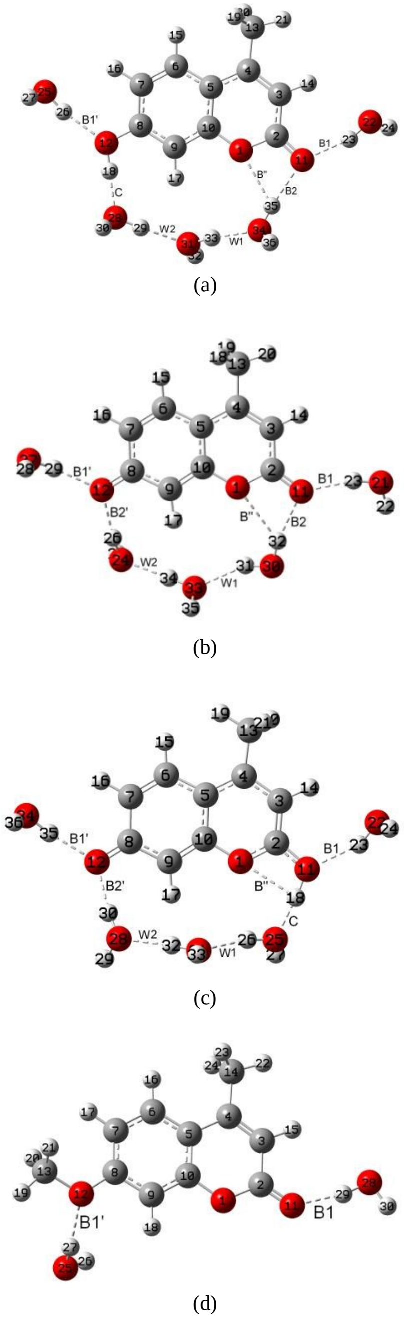

Fig. 1. S_0 state optimized structure of (a) 4MU-$(H_2O)_5$ (b) $4MU^-$-$(H_2O)_5$ (c) 4MUPT-$(H_2O)_5$ and (d) MMC-$(H_2O)_2$ molecules.

In the case of 4MU, $4MU^-$ and 4MUT molecule, there are at least five sites for HB formation with protic solvent molecules as shown in Fig. 1; two intermolecular HB C=O···H (B type) by oxygen of the carbonyl group with hydrogen of a water

Cite this: DOI: 10.1039/c0xx00000x

www.rsc.org/xxxxxx

molecules, one C-O···H (B′ type) between oxygen of hydroxyl group and hydrogen of water molecule, one HB (B″ type) by oxygen of the pyrone ring with hydrogen of hydroxyl group or water molecule and one HB O-H···O (type C) via the participation of hydroxyl hydrogen atom with oxygen atom of water molecule. $4MU^-$ can also form five HBs; two B type, two B′ type and one B″ type. The MMC molecule can form only two HBs; one B type and one B′ type.

In this work, we implement the EFP1 method of solvation for explicit water molecules interfaced with the PCM model. We demonstrate the possibility of ESHT in 4MU in the S_1 state rather than the ESPT. Here, the occurrence of ESHT in 4MU has been reported on the basis of electronic structure, simulated TDDFT spectra and change in HB energies (ΔE_{HB}'s) as a result of the $S_0 \rightarrow S_1$ transition using TDDFT/PCM/EFP1 method.

Computational methods

A small cluster of 10 EFP[24] water molecules were added to hydrogen bonding sites of monomers and optimized with the MMFF94s force field using Avogadro software. Enol and keto tautomers of 4MU, and $4MU^-$ formed four HBs along with HB network between carbonyl and hydroxyl groups using five water molecules. The MMC molecule formed only two HBs with water molecules. Hydrogen bonded water molecules along with the HB network are used to form water complexes of monomers. The optimization of the 4MU molecule, $4MU\text{-}(H_2O)_5$, $4MUT\text{-}(H_2O)_5$ and $4MU^-\text{-}(H_2O)_5$ complexes have been performed at the DFT level[25,26] using B3LYP[27] hybrid function with 6-31G(d,p)[28] basis set. MMC and $MMC\text{-}(H_2O)_2$ molecules were also optimized with same level of theory using cc-pVDZ[29] basis set. The geometries of the first singlet excited state were optimized using the state specific TD-B3LYP[30] method with same basis set based on the optimized ground state geometry. SS-TDDFT/PCM/EFP1 method[31] with CAM-B3LYP[32] functional for 4MU water complexes[33] and B3LYP functional for MMC and its water complex were used to compute transition energies. The relaxed geometry of the first excited state is used to calculate the fluorescence spectra. The explicit water molecules are treated as EFPs for DFT and TDDFT calculations. Natural atomic orbital and Natural bond orbital analysis have been carried out to calculate charge on each atom at S_0 and S_1 states using the NBO 6.0[34] package. All calculations were performed using the GAMESS-US software suit.[35]

The HB energy is computed by equating interaction energy between solute and solvent molecules.[36] The optimized geometry of complexes is used to compute the energy of free solute, E_{solu} by removing solvent molecules from the system. Then, the solvent-solute interaction energy, (E_{HB}) is calculated as

$$E_{HB} = E_{complex} - (E_{solu} + E_{solv}) \qquad (1)$$

where $E_{complex}$ is total energy of the complex and E_{solv} is total EFP energy. By calculating E_{HB} at both S_0 and S_1 states, the change in HB energy can be obtained as

$$\Delta E_{HB} = (E_{HB})_{S1} - (E_{HB})_{S0} \qquad (2)$$

From the optimized geometry of a complex, all other water molecules are removed except one water molecule which forms a respective type of HB, and its energy is calculated using equation (1) with the same scheme.

Results and discussion

Electronic structure in ground state

The S_0 state optimized structures of $4MU\text{-}(H_2O)_5$, $4MU^-\text{-}(H_2O)_5$, $4MUT\text{-}(H_2O)_5$ and $MMC\text{-}(H_2O)_2$ molecules are shown in Fig. 1. In all complexes, the carbonyl and hydroxyl groups lie in the same plane. From Fig. 1a and 1c, one can clearly see that two C=O---H-O (B type) HBs are formed between the oxygen atom of the carbonyl group and the hydrogen atom of water molecules, one HB C-O···H (B′ type) formed between oxygen of hydroxyl group and the hydrogen of a water molecule, one HB (B″ type) by oxygen of the pyrone ring with hydrogen of water molecule/ hydroxyl group and one HB O-H···O (type C) by hydroxyl hydrogen atom with oxygen atom of a water molecule. In $4MU^-$ (Fig. 1b) the oxygen atom of the carbonyl group forms two B type HBs, oxygen of hydroxyl group form two B′ type HBs and oxygen of the pyrone ring form one B″ type HB. Similarly, carbonyl and hydroxyl oxygen of the MMC molecule form one B type and one B′ type HBs respectively, with hydrogen of the water molecules. In addition to these HBs, there is also formation of two HBs (W type) between water molecules in 4MU complexes.

From optimized geometry bond lengths and bond angles of both 4MU and MMC monomers in the S_0 state and $4MU\text{-}(H_2O)_5$, $4MUT\text{-}(H_2O)_5$, $4MU^-\text{-}(H_2O)_5$ and $MMC\text{-}(H_2O)_2$ complexes in the S_0 and S_1 states are calculated and displayed in Table 1. The formation of HBs slightly changes the structure of 4MU. The O1-C2 bond length in pyrone ring decreased by 0.025 Å, C2=O11 bond length of the carbonyl group increased by 0.021 Å due to the formation of B type HBs, C8-O12 bond length decreased by 0.012 Å and O12-H18 bond length of the hydroxyl group increased by 0.004 Å due to B′ and C type HBs. In $MMC\text{-}(H_2O)_2$ complex, the O1-C2 bond length decreased by 0.009 Å, the C2=O11 bond length increased by 0.006 Å due to the formation of B type HB and the C8-O12 bond length increased by 0.003 Å due to B′ type HBs. The change in other bond lengths and bond angles are less than 0.008 Å and 1.5°, respectively.

Electronic structure in the excited state

In the S_1 state of $4MU\text{-}(H_2O)_5$ and $MMC\text{-}(H_2O)_2$ complexes O1-C2, C3-C4, C2=O11, C4-C5, C5-C6, C5-O10, C7-C8 bond lengths increase, whereas O1-C10, C2-C3, C4-C(13,14) bond lengths decrease. Similar changes in bond lengths are observed due to molecular excitation of 4MUT-(H$_2$O)$_5$ and 4MU^{-}-(H$_2$O)$_5$ complexes except C2-C3, C3-C4, C5-C6, C5-C10, C7-C8, C8-C9 and C8-O12 bonds as compared to 4MU-(H$_2$O)$_5$ complex. In the S$_1$ state, the bond angle C2-O1-C10 altered by 14.1° in the 4MU-(H$_2$O)$_5$ complex due to strengthening of B′ type HB. All other bond angles in 4MU-(H$_2$O)$_5$, all bond angles in 4MUT-(H$_2$O)$_5$, 4MU^{-}-(H$_2$O)$_5$ and MMC-(H$_2$O)$_2$ complexes are distorted by 1- 4°. The ground and excited state HB lengths of complex molecules are displayed in Table 2 along with C-O($^{-}$H,CH3) and O-H bond lengths. As can be seen in the Table 2, due to molecular excitation, the B′ type HB elongates in 4MU-(H$_2$O)$_5$, 4MU^{-}-(H$_2$O)$_5$ and MMC-(H$_2$O)$_2$ complexes, whereas in 4MUT-(H$_2$O)$_5$ complex one B′ type HB elongated and other get contracted. B type HB length increases in 4MU-(H$_2$O)$_5$, MMC-(H$_2$O)$_2$ complexes and decreases in 4MU^{-}-(H$_2$O)$_5$, 4MUT-(H$_2$O)$_5$, complexes. In the S$_1$ state of 4MU-(H$_2$O)$_5$ complex, O-H bond length increases and C-OH bond length decreases due to strengthening of C type HB, whereas O-H bond length decreases and C-OH bond length increases in 4MUT-(H$_2$O)$_5$ complex due to weakening of C type HB. C-O^{-} bond length increases in 4MU^{-}-(H$_2$O)$_5$ complex and C=O bond length increases in all complexes. In 4MU-(H$_2$O)$_5$ complex W type HBs contracted, whereas in 4MU^{-}-(H$_2$O)$_5$ and 4MUT-(H$_2$O)$_5$ complexes one W type HB stretched out and other gets contracted.

Table 1. Selected bond lengths, r (Å) and bond angles, A (º) in the S$_0$ and S$_1$ state.

r/A	4MU	4MU-(H$_2$O)$_5$		4MU^{-}-(H$_2$O)$_5$		4MUT-(H$_2$O)$_5$		MMC	MMC-(H$_2$O)$_2$	
	S$_0$	S$_0$	S$_1$	S$_0$	S$_1$	S$_0$	S$_1$	S$_0$	S$_0$	S$_1$
R(1-2)	1.402	1.377	1.509	1.363	1.425	1.337	1.356	1.401	1.392	1.448
R(1-10)	1.362	1.368	1.351	1.373	1.351	1.383	1.355	1.363	1.364	1.344
R(2-3)	1.456	1.442	1.429	1.434	1.424	1.374	1.410	1.456	1.454	1.419
R(2-11)	1.206	1.227	1.229	1.224	1.244	1.316	1.328	1.207	1.213	1.224
R(3-4)	1.361	1.367	1.385	1.366	1.379	1.417	1.371	1.361	1.362	1.416
R(4-5)	1.454	1.447	1.482	1.424	1.500	1.400	1.498	1.454	1.454	1.431
R(4-13/14)	1.505	1.505	1.495	1.504	1.487	1.505	1.488	1.505	1.504	1.497
R(5-6)	1.410	1.414	1.393	1.417	1.419	1.438	1.425	1.407	1.408	1.421
R(5-10)	1.415	1.408	1.449	1.412	1.389	1.435	1.381	1.416	1.415	1.463
R(6-7)	1.389	1.384	1.399	1.367	1.389	1.365	1.383	1.392	1.392	1.396
R(7-8)	1.409	1.414	1.433	1.446	1.430	1.463	1.439	1.410	1.408	1.424
R(8-9)	1.396	1.396	1.393	1.428	1.443	1.440	1.446	1.400	1.400	1.404
R(8-12)	1.360	1.348	1.338	1.268	1.285	1.259	1.271	1.359	1.362	1.356
R(9-10)	1.395	1.387	1.394	1.369	1.417	1.360	1.418	1.392	1.392	1.390
R(12/11-18/13)	0.969	0.973	0.980	-	-	0.988	0.982	1.422	1.429	1.431
A(2-1-10)	122.1	122.6	108.5	123.0	120.8	121.2	119.4	122.1	121.9	120.8
A(1-2-3)	116.0	117.1	112.5	117.3	116.4	122.1	121.5	116.2	116.9	117.4
A(1-10-5)	121.9	121.2	118.2	120.1	124.2	119.4	123.5	121.9	121.8	121.8
A(2-3-4)	123.3	122.0	122.4	121.6	124.9	119.2	121.0	123.3	122.7	123.5
A(3-4-5)	118.5	119.3	113.3	119.8	116.2	119.7	117.1	118.5	118.7	117.3
A(4-5-10)	118.0	117.8	117.5	118.2	117.6	118.4	117.4	118.1	118.1	119.0
A(6-5-10)	117.3	116.4	117.1	115.8	116.8	114.7	115.7	117.3	117.1	116.3
A(5-6-7)	121.5	121.8	121.3	122.1	123.8	122.1	123.9	122.0	122.0	121.8
A(5-10-9)	121.9	123.1	122.2	123.6	121.5	124.7	123.1	121.6	121.8	121.7
A(6-7-8)	119.8	119.8	120.3	122.0	120.1	122.1	120.7	119.4	119.4	120.3
A(7-8-9)	120.2	119.9	119.7	115.5	116.4	115.6	115.7	119.9	120.0	119.7
A(8-9-10)	119.3	118.9	119.1	121.0	121.4	120.4	120.7	119.7	119.6	120.1
A(8-12-13)	-	-	-		-	-	-	118.6	118.9	119.7

Table 2. C=O, C-O($^{-}$,H,CH3), O-H and HB lengths, r$_{HB}$ (Å) in the S$_0$ and S$_1$ states.

r	4MU-(H$_2$O)$_5$		4MU^{-}-(H$_2$O)$_5$		4MUT-(H$_2$O)$_5$		MMC-(H$_2$O)$_2$	
	S$_0$	S$_1$	S$_0$	S$_1$	S$_0$	S$_1$	S$_0$	S$_1$
C-O($^{-}$, H,CH3)	1.348	1.338	1.268	1.284	1.316	1.328	1.362	1.356
O-H(CH3)	0.973	0.980	-	-	0.988	0.982	1.429	1.431
C=O	1.227	1.230	1.224	1.245	1.259	1.272	1.213	1.224
C=O---H (B1 type)	1.846	1.854	1.818	1.804	1.899	1.887	1.870	1.876
C=O---H (B2 type)	1.916	2.017	1.971	1.884	-	-	-	-
C-O---H (B1′ type)	1.860	1.888	1.780	1.809	1.810	1.820	1.908	1.957
C-O---H (B2′ type)	-	-	1.759	1.773	1.815	1.806	-	-
O---H (B″ type)	2.091	1.934	2.291	2.381	2.179	2.219	-	-
O-H---O (C type)	1.635	1.533	-	-	1.523	1.555	-	-
W1	1.761	1.694	1.951	2.024	1.748	1.755	-	-
W2	1.744	1.680	1.770	1.768	1.777	1.763	-	-

Charge transfer indexes

In order to explore the charge transfer and change in HB length, the natural charges by NBO analysis of 4MU-(H$_2$O)$_5$ and MMC-(H$_2$O)$_2$ complexes in the S$_0$ and S$_1$ state have been computed using the CAM-B3LYP functional. The frontier molecular orbitals (MOs) of 4MU and MMC molecules are computed at the B3LYP level, depicted graphically in Fig. 2 along with the charge density (ρ) variation upon excitation, the blue and red zones are corresponding to ρ_{+} and ρ_{-}, respectively. In both complexes, upon excitation, the density depletion zones (red) are located on C2, C4, C6, C8 and C9 atoms, whereas the regions of density increment (blue) localized on C3, C5, C7, C10, O11 and O12 atoms. The change of natural charges on various atoms and groups due to excitation is listed in Table 3. The natural charges on the O1 atom decreases in 4MU-$(H_2O)_5$ and increases in MMC-$(H_2O)_2$ complexes. The increase in natural charge on O11 and O12 atoms accounts for the weakening of B and B′ type HBs. In 4MU-$(H_2O)_5$ complex the natural charge on the H18 atom increases in the S_1 state. This causes the strengthening of C type HB. The increase in natural charge on O12 and H18 atoms at the excited state of 4MU-$(H_2O)_5$ indicates the possibility of hydrogen transfer in the excited state.

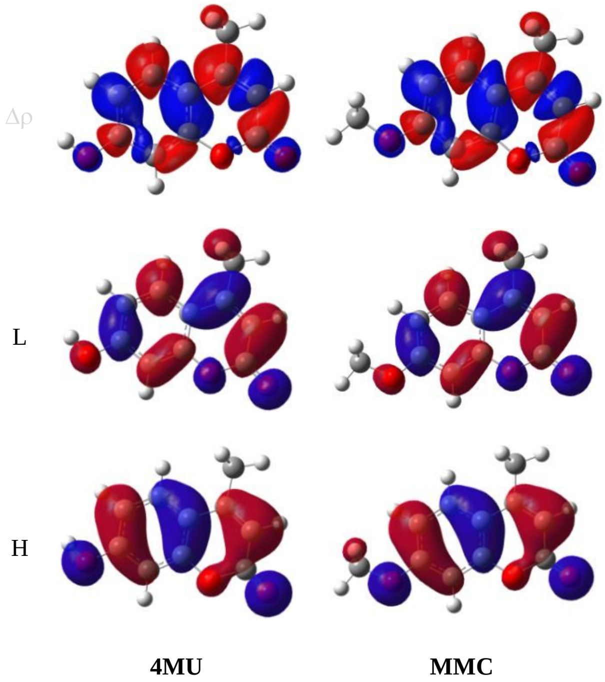

Fig. 2 Molecular orbitals (H-HOMO, L-LUMO) and difference charge density (Δρ, blue-ρ_+ and red-ρ_-) plot ($S_0 \rightarrow S_1$) of 4MU and MMC molecules.

Table 3. Change of natural charges on excitation ($S_0 \rightarrow S_1$), Δ*e* of 4MU and MMC molecules in their complexes.

Atom	4MU	MMC	Atom/group	4MU	MMC
O1	-0.013	0.009	O11	0.011	0.018
C2	-0.080	-0.058	O12	0.046	0.033
C3	0.042	0.008	4-CH3	0.010	0.007
C4	-0.152	-0.107	H14(15)	-0.006	-0.004
C5	0.161	0.125	H15(16)	0.008	0.005
C6	-0.069	-0.094	H16(17)	0.003	0.001
C7	0.062	0.086	H17(18)	0.006	0.003
C8	-0.004	-0.015	H18	0.006	-
C9	-0.003	-0.026	CH3(-O)	-	0.024
C10	0.008	0.032			

From Fig. 2 it can also be observed that the intramolecular redistribution of electronic charges occurs from the hydroxyl group and benzene ring to pyrone ring of coumarin moiety. Thus, the excited state of 4MU and MMC molecules may be an ICT state.

Electronic spectra and the excited state properties

We simulate the real time TD absorption spectrum originating from the first excited state of 4MU-$(H_2O)_5$, $4MU^{-}$-$(H_2O)_5$ and 4MUT-$(H_2O)_5$, complexes by applying TD-CAM-B3LYP/PCM/EFP1 calculations. The first excitation energies of MMC and MMC-$(H_2O)_2$ complex are calculated at TD-B3LYP/PCM/EFP1 level. The absorption energy with corresponding oscillation strengths in gas phase and in solvents in the S_1 state are listed in Table 4. The assignments of the electronic excitations in Table 4 reveals that the major contributions (~ 95%) of the orbital transitions in the S_1 state come from H → L for all molecules.

Table 4. Absorption energy ($S_0 \rightarrow S_1$), E_a (eV), oscillator strength, f and assignment of electronic excitations of 4MU-$(H_2O)_5$, $4MU^{-}$-$(H_2O)_5$, 4MUT-$(H_2O)_5$, MMC and MMC-$(H_2O)_2$ molecules in gas phase and in solvents. Only selected transitions with enough oscillator strength around the main peak are included.

Molecule	Solvent/ gas phase	E_a (eV)	f	Wave function (excitation amplitude)
4MU-$(H_2O)_5$	Gas phase	4.21	0.355	H → L (0.967) H – 1 → L + 1 (0.170)
	Water	4.18	0.433	H → L (0.973) H – 1 → L + 1 (0.147)
$4MU^{-}$-$(H_2O)_5$	Gas phase	3.71	0.395	H → L (0.983) H – 1 → L + 1 (0.121)
	Water	3.73	0.484	H → L (0.984) H – 1 → L + 1 (0.103)
4MUT-$(H_2O)_5$	Gas phase	3.46	0.370	H → L (0.974) H – 2 → L (0.145) H – 2 → L + 1 (0.124)
	Water	3.47	0.455	H → L (0.980) H – 2 → L (0.100) H – 2 → L + 1 (0.100)
MMC	Gas phase	4.14	0.315	H → L (0.956) H – 2 → L (0.145) H – 2 → L + 1 (0.124)
	Water	3.85	0.662	H → L (0.991)
	Methanol	3.86	0.653	H → L (0.991)
MMC-$(H_2O)_2$	Gas phase	4.17	0.324	H → L (0.958) H – 1 → L (0.138) H – 1 → L + 1 (0.186) H – 1 → L + 2 (0.120)
	Water	4.06	0.428	H → L (0.979) H – 1 → L + 1 (0.141)

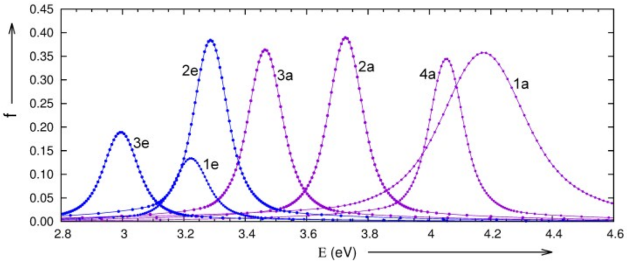

Fig. 3 Simulated real-time TD-DFT absorption (violet) and emission (blue) spectra of 4MU (1a, 1e), $4MU^{-}$ (2a,2e), 4MUT (3a,3e) and MMC (4a) complexes in water

The TD-CAM-B3LYP/PCM/EFP1 calculations of 4MU-$(H_2O)_5$ complex shows the absorption maxima at 4.21 eV in gas phase and 4.18 eV in water (Fig. 3). The absorption maxima of MMC in gas phase, water and methanol are found to be 4.14, 3.85 and

3.86 eV, respectively, whereas the absorption maxima of MMC-$(H_2O)_2$ in gas phase and water are found to be 4.17 and 4.06 eV, respectively. The experimentally determined value of absorption energy for 4MU in water is 3.88 eV[37] (3.85 eV[38]) and MMC in methanol is 3.88 eV.[38] In our calculation, the deviation 0.30 eV for 4MU and 0.02 eV for MMC from experimental values may be due to the use of non diffuse basis sets to minimize computational cost. The TD-CAM-B3LYP/PCM/EFP1 calculation using 6-31+G(d,p) basis set for 4MU in water produces the redshift of 0.1 eV in its absorption maximum compared with the calculation using 6-31G(d,p) basis set. Fluorescence spectra of 4MU-$(H_2O)_5$, $4MU^-$-$(H_2O)_5$ and 4MUT-$(H_2O)_5$ complexes in water from their relaxed geometry of the first excited state, calculated at TD-CAM-B3LYP/PCM/EFP1 level produce emission energies 3.23, 3.31 and 3.0 eV respectively. The Stokes' shift between absorption energy of 4MU and emission energy of 4MU, $4MU^-$, 4MUT are calculated as 0.95, 0.87 and 1.18 eV. The experimental value of stokes' shift is found to be 1.12 eV,[37] which is in good agreement with the Stokes' shift produced by the absorption energy of 4MU and emission energy of 4MUT complexes in water (5.1% deviation). The Stokes' shift calculated for C152 by A Pedone[33] with the same level of theory produces the result with deviation of 5.5% from the experimental value. This confirms the hydrogen transfer state of 4MU in the S_1 state.

The ground state and excited state energy of $4MU^-$-$(H_2O)_5$ is about 13 eV higher than the 4MU-$(H_2O)_5$ and 4MUT-$(H_2O)_5$ complexes. Hence, the formation of $4MU^-$ either in S_0 or S_1 state is not probable.

Table 5. Hydrogen bond energy, E_{HB} (kJ/mol) and ΔE_{HB} of 4MU-$(H_2O)_5$, 4MUT-$(H_2O)_5$ and MMC-$(H_2O)_2$ complexes.

Type of HB	4MU-$(H_2O)_5$			4MUT-$(H_2O)_5$			MMC-$(H_2O)_2$		
	$(E_{HB})_{S0}$	$(E_{HB})_{S1}$	ΔE_{HB}	$(E_{HB})_{S0}$	$(E_{HB})_{S1}$	ΔE_{HB}	$(E_{HB})_{S0}$	$(E_{HB})_{S1}$	ΔE_{HB}
B, B′, (C)	-276.39	-281.74	5.35	-303.37	-288.19	-15.18	-78.37	-74.77	-3.60
B1	-45.27	-45.56	0.28	-35.03	-37.60	2.58	-41.20	-42.05	0.85
B2	-45.51	-46.26	0.75	-	-	-	-	-	-
B1'	-40.41	-38.53	-1.87	-54.29	-49.47	-4.82	-37.22	-33.12	-4.10
B2'	-	-	-	-50.69	-47.12	-3.56			
C	-55.83	-60.20	4.37	-76.14	-65.16	-10.98	-	-	-
W1+W2	-23.69	-23.36	-0.33	-23.35	-23.37	0.02	-	-	-

Hydrogen bond dynamics

TDDFT computations of 4MU-$(H_2O)_5$, 4MUT-$(H_2O)_5$ and MMC-$(H_2O)_2$ complexes for their respective type of HB have been carried out by infinitely separating the other water molecules, and ΔE_{HB}'s are calculated using Eq.1 and Eq.2. The ΔE_{HB} for W type HBs were estimated by calculating the EFP/PCM electrostatic interactions in the S_0 and S_1 state. The electronic excitation energies corresponding to the $S_0 \rightarrow S_1$ transition for B, B′ and C type HBs were calculated using the TDDFT/PCM/EFP1 method and presented in Table 5. In the S_1 state of all complexes, B type intermolecular HBs strengthened, whereas B′ type intermolecular HBs are weakened. In 4MU-$(H_2O)_5$ complex ΔE_{HB} increases for C type HB. The ΔE_{HB} of W type HBs can be scorned compared to ΔE_{HB} of the other type of HBs. In 4MU-$(H_2O)_5$ complex, B and C type HB energy increased by 1.03 and 4.37 kJ/mol, respectively whereas B′ type HB energy decreased by 1.87 kJ/mol.

The total (sum of A, B1, B2 and C types) change in HB energy is found to be 2.15 kJ/mol lesser than the change in HB energy of 4MU-$(H_2O)_5$ complex. In 4MUT-$(H_2O)_5$ complex, ΔE_{HB} of B type HBs increased by 2.58 kJ/mol, whereas ΔE_{HB} of B′ and C type HBs decreased by 8.38 and 10.98 kJ/mol, respectively. The change in HB energy of 4MUT-$(H_2O)_5$ complex is found to be 1.58 kJ/mol higher than the sum of HB energy of B, B′ and C type HBs. In MMC-$(H_2O)_2$ complex, B type HB strengthened by 0.85 kJ/mol, whereas B′ type HB weakened by 4.10 kJ/mol, respectively. The change in HB energy of MMC-$(H_2O)_2$ complex is 3.60 kJ/mol, which is equal to sum of HB energy of B and B′ types within the limit of calculation error 0.35 kJ/mol. The change in HB energy calculated for 4MU-$(H_2O)_5$ and 4MUT-$(H_2O)_5$ molecules shows discrepancy compared with the sum of HB energies of A, B, B′ and C types. This indicates there may be different types of HBs in the S_0 and S_1 states of 4MU-$(H_2O)_5$ and 4MUT-$(H_2O)_5$ molecules. The ground state energy of 4MUT is 0.89 eV higher than the S_0 state energy of 4MU, which indicates the nonexistence of 4MUT in the S_0 state. So, we can expect different structure of 4MU-$(H_2O)_5$ complex in the excited state.

Excited state hydrogen transfer character

In pursuance of hydrogen transfer in the excited state, we focused on the calculations of ΔE_{HB} between 4MU-$(H_2O)_5$ complex in the ground state and 4MUT-$(H_2O)_5$ complex in the excited state, as reported in Table 6. The total change in HB energy is equal to sum of ΔE_{HB}'s of all HBs within the limit of calculation error 0.21 kJ/mol.

Table 6. Hydrogen bond length r_{HB} (Å) energy, E_{HB} (kJ/mol) and ΔE_{HB} of 4MU-$(H_2O)_5$ complex at S_0 state and 4MUT-$(H_2O)_5$ complex in the S_1 state.

Type of HB	4MU-$(H_2O)_5$		4MUT-$(H_2O)_5$		ΔE_{HB}
	$(r_{HB})_{S0}$	$(E_{HB})_{S0}$	$(E_{HB})_{S1}$	$(r_{HB})_{S1}$	
B, B′, C	-	-276.39	-288.19	-	11.80
B1	1.846	-45.27	-37.60	1.887	-7.67
B2	1.916	-45.51	-	-	-45.51
B1'	1.860	-40.41	-49.47	1.820	9.06
B2'	-	-	-47.12	1.806	47.12
C	1.635	-55.83	-65.16	1.555	9.33
W1+W2	-	-23.69	-23.37	-	-0.32

Upon excitation of 4MU-$(H_2O)_5$ complex and de-excitation of 4MUT-$(H_2O)_5$ complex, C-OH and O-H···O HB lengths decreases, whereas O-H bond length increases (Table 2). Thus, the hydrogen atom may release from the hydroxyl group due to excitation of 4MU-$(H_2O)_5$ and de-excitation of 4MUT-$(H_2O)_5$ in water. So, in the S_1* state, 4MU get transferred to 4MUT and vice versa in the S_0* state.

To comprehend the mechanism of hydrogen transfer, potential energy curves have been scanned by keeping the O-H distance fixed with series of values from 0.65 to 1.3 Å in the S_0 and S_1

states of 4MU-$(H_2O)_5$ and 4MUT-$(H_2O)_5$ complexes using the TD-CAM-B3LYP/PCM/EFP1 method and displayed in Fig. 4. The plot of potential energy curves provides the qualitative energetic pathway for the ESHT process of the 4MU chromophore. One should be noted that there is a high barrier (about 0.89 eV) in the S_0 state between 4MU and 4MUT, due to which hydrogen transfer is least probable in ground state.

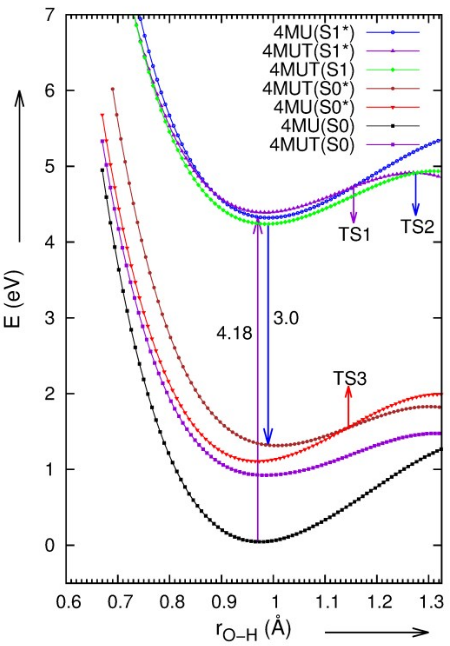

Fig. 4 The potential energy curves along O-H bond for the ground and first excited states of 4MU and 4MUT complexes in water.

However, it should be noted that the S_1 state potential energy curves exhibits a very low barrier of 0.07 eV between the 4MU and 4MUT in the S_1* state, and cross over at TS1, where phototautomerization can occur. Further, the transition of 4MUT from S_1* to S_1 state transpire at the cross over TS2. Therefore, hydrogen transfer is more likely to be proceeded in the excited state. Subsequently, the 4MUT decays to S_0* state through radiating fluorescence with 3.0 eV peak and can undergo reverse ground state hydrogen transfer process at the cross over TS3 of potential energy curves.

The change in HB energy between 4MU-$(H_2O)_5$ complex in the ground state and 4MUT-$(H_2O)_5$ complex in the excited state, stretching of OH bond, fluorescence spectral studies and potential energy curves along OH bond confirms the formation of 4MUT-$(H_2O)_5$ complex in the excited state. The proposed excited state hydrogen transfer scheme is presented in Fig. 5.

Conclusion

In summary, here we applied TDDFT/EFP1 protocol for the characterization of hydrogen bond energy in the S_0 and S_1 state of 4-Methylumbelliferone, its phototautomer and 7-methoxy-4-methylcoumarin along with the electronic structure, spectral properties and excited state hydrogen transfer character in 4-Methylumbelliferone. Our calculated value of Stokes' shift based on the TD-CAM-B3LYP/PCM/EFP1 method is in good agreement with the experimental result. The strengthening of O-H···O hydrogen bond and weakening of the O-H bond in the S_1 state indicated the tendency of excited state hydrogen transfer. The corresponding frontier molecular orbitals and the charge density variation upon excitation, have been analyzed manifesting the excited state hydrogen transfer process could happen due to the intramolecular charge transfer.

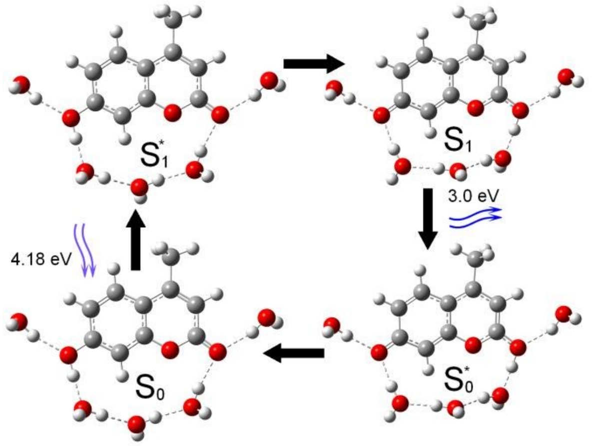

Fig. 5 Proposed hydrogen transfer scheme for 4MU in water.

The constructed potential energy curves of the S_0 state and S_1 state demonstrate that the hydrogen transfer is more likely to happen in the excited state due to the relatively lower barrier. From a mechanistic point of view, our results clearly show that the overall driving force for the hydrogen transfer is due to intramolecular charge transfer and strengthening of O-H···O hydrogen bond.

Acknowledgement

This work was supported by the University Grants Commission, India under the research project No. 1502-MRP/14-15/KAMY022/UGC-SWRO.

Notes and references

[a] *PG Department of Physics, Govt. College, (Autonomous), Mandya - 571401, INDIA. E-mail: hmrgowda@yahoo.com.*

1 N. H. March, M. P. Tosi, Coulomb Liquids, Academic Press, New York, 1984.
2 a) L. Bicz_k, T. B_rces, H. Linschitz, *J. Am. Chem. Soc.*. 1997, **119**, 11 071; b) R. S. Moog, N. A. Burozski, M. M. Desai, W. R. Good, C. D. Silvers, P. A. Thomson, J. D. Simon, *J. Phys. Chem*., 1991, **95**, 8466; c) D. K. Palit, T. Zhang, S. Kumazaki, K. Yoshihara, *J. Phys. Chem. A*, 2003, **107**, 10789; d) C. Chudoba, E. T. J. Nibbering, T. Elsaesser, *J. Phys. Chem. A*, 1999, **103**, 5625; e) A. Demeter, L. Barasz, T. B_rces, *J. Phys. Chem. A*, 2004, **108**, 4357.
3 a) Y. Liu, J. Ding, R. Liu, D. Shi, J. Sun, *J. Photochem. Photobiol. A*, 2009, **201**, 203; b) P. Zhou, P. Song, J. Liu, K. Han, G. He, *Phys. Chem. Chem. Phys*., 2009, **11**, 9440; c) Y. Liu, J. Ding, D. Shi, J. Sun, *J. Phys. Chem. A*, 2008, **112**, 6244; d) M. Miao, Y. Shi, *J. Comput. Chem*., 2011, **32**, 3058; e) Y. H. Liu, P. Li, *J. Lumin*., 2011, **131**, 2116; f) E. Pines, D. Pines, Y. Z. Ma, G. R. Fleming, *ChemPhysChem*, 2014, **9**, 1315; g) E. T. J. Nibbering, H. Fidder, E. Pines, *Annu. Rev. Phys. Chem*., 2005, **56,** 337; h) G. J. Zhao, K. L.Han, *Acc. Chem. Res*., 2012, **45**, 404; i) G. J. Zhao, K. L. Han, *J. Phys. Chem. A*, 2007, **111**, 9218; j) W. Zhao, L. Pan, W. Bian, J. Wang, *ChemPhysChem*, 2008, **9**, 1593; k) G. J. Zhao, J. Y. Liu, L. C. Zhou, K. L. Han, *J. Phys. Chem. B*, 2007, **111**, 8940; l) M. Zhang, B. Ren, Y. Wang, C. Zhao, *Spectrochimica Acta Part A*, 2013, **101**, 191.

4 a) M. Ramegowda, *New J. Chem*., 2013, **37**, 2648; b) M. Ramegowda, *Res. J. Chem. Sci*., 2013, **3(7)**, 1; c) M. Ramegowda, *Spectrochimica Acta Part A*, 2015, **137**, 99; d) G. J. Zhao, K. L. Han, *ChemPhysChem*, 2008, **9**, 1842; e) G. J. Zhao, K. L. Han, *J. Phys. Chem. A*, 2007, **111**, 2469; f) Hydrogen Bonding, Transfer in the Excited State. K.L. Han, G.J. Zhao, John Wiley & Sons Ltd, 2011; g) Y. H. Liu, S. C Lan, *Commun. Comput. Chem*., 2013, **1**, 1; h) G. Y. Li , Y. H. Li, H. Zhang, G.H Cui, *Commun. Comput. Chem*., 2013, **1**, 88; i) G. J. Zhao, K. L. Han, *Biophys.J*., 2008, **94**, 38; j) T. Kowalczyk, S. R. Yost, T. Van Voorhis, *J. Chem. Phys*., 2011, **134**, 054128; k) M. W. D. Hanson-Heine, A. Wriglesworth, M. Uroos, J. A. Calladine, T. S. Murphy, M. Hamilton, I. P.Clark, M. Towrie, J. Dowden, N. A. Besley,M. W. George, *J. Chem. Phys*., 2015, **142**, 154119.

5 a) A. Morimoito, T. Yatsuhashi, T. Shimada, L. Biczok, D. A. Tryk, H. Inoue, *J. Phys. Chem. A*, 2001, **105**, 10488; b) L. Biczok, T. Berces, H. Linschitz, *J. Am. Chem. Soc*., 1997, **119**, 11071; c) V. Vetokhina, M. Kijak, G. Wiosna-Salyga, R. P. Thummel, J. Herbich, J. Waluk, *Photochem. Photobiol. Sci*., 2010, **9**, 923; d) A. Kyrychenko, J. Waluk, *J. Phys. Chem. A*, 2006, **110**, 11958; e) J. Waluk, *Acc. Chem. Res*., 2003, **36**, 832; f) E. Krystkowiak, A. Maciejewski, *Phys. Chem. Chem. Phys*., 2011, **13**, 11317.

6 a) G. Jones II, W. R. Jackson, A. M. Halpern, *Chem. Phys. Lett*., 1980, **72**, 391; b) M. J. Kamlet, C. Dickinson, R. W. Taft, *Chem. Phys. Lett*., 1981, **77**, 69; c) V. Masilamani, B. M. Sivaram, *J. Lumin*., 1982, **27**, 147; d) T. L. Arbeloa, F. L. Arbeloa, M. J. Tapia, I. L. Arbeloa, *J. Phys. Chem*., 1993, **97**, 4704; e) T. L. Arbeloa, F. L. Arbeloa, M. J. Tapia Estevez, I. L. Arbeloa, *J. Lumin*., 1994, **59**, 369.

7 a) E. Krystkowiak, K. Dobek, A. Maciejewski, *J. Photochem. Photobiol., A*, 2006, **184**, 250; b) K. Matsubayashi, Y. Kubo, *J. Org. Chem*., 2008, **73**, 4915; c) V. Samant, A. K. Singh, G. Ramakrishna, H. N. Ghosh, T. K. Ghanty, D. K. Palit, *J. Phys. Chem. A*, 2005, **109**, 8693; d) M. A. Munoz, M. Galan, L. Gomez, C. Carmona, P. Guardado, M. Balon, *J. Chem. Phys*., 2003, **290**, 69; e) C. Carmona, M. Balon, M. Galan, P. Guardado, M. A. Munoz, *Photochem. Photobiol*., 2002, **76**, 239; f) C. Carmona, M. Balon, M. Galan, G. Angulo, P. Guardado, M. A. Munoz, *J. Phys. Chem. A*, 2001, **105**, 10334.

8 a) P. N. Day, J. H. Jensen, M. S. Gordon, S. P. Webb, W. J. Stevens, M. Krauss, D. Garmer, H. Basch, D. Cohen, *J. Chem. Phys*. 1996, **105**, 1968; b) M. S. Gordon, M. A. Freitag, P. Bandyopadhyay, J. H. Jensen, V. Kairys, W. J. Stevens, *J. Phys. Chem. A*, **105**, 293; c) I. Adamovic, M. A. Freitag, M. S. Gordon, *J. Chem. Phys*., 2003, **118,** 6725; d) J. H. Jensen, M. S. Gordon, *J. Chem. Phys*., 1998, **108**, 4772.

9 P. Arora, L. V. Slipchenko, S. P. Webb, A. DeFusco, M. S. Gordon, *J. Phys. Chem. A*, 2010, **114**, 6742.

10 N. Minezawa, N. De Silva, F. Zahariev, M. S. Gordon, *J. Chem. Phys*., 2011, **134**, 54111.

11 S. Yoo, F. Zahariev, S. Sok, M. S. Gordon, *J. Chem. Phys*., 2008, **129**, 144112.

12 a) C. W. Hoganson, G. T. Babcock, *Science*, 1997, **277**, 1953; b) J. B. Howard, D. C. Rees, Proc. *Natl. Acad. Sci. U.S.A*., 2006, **103**, 17088; c) D. R. Weinberg, C. J. Gagliardi, J. F. Hull, C. F. Murphy, C. A. Kent, B. C. Westlake, A. Paul, D. H. Ess, D. G. McCafferty, T. J. Meyer, *Chem. Rev*., 2012, **112**, 4016; d) M. Meyer, J. Klinman, *J. Chem. Phys*., 2005, **319**, 283; e) B. Li, J. Zhao, K. Onda, K. Jordan, J. Yang, H. Petek, *Science*, 2006, **311**, 1436.

13 a) T. Meyer, M. Huynh, H. Thorp, *Angew. Chem., Int. Ed*., 2007, **46**, 5284; b) C.-C. Hsieh, Y.-M. Cheng, C.-J. Hsu, K.-Y. Chen, P.-T. Chou, *J. Phys. Chem. A*, 2008, **112**, 8323; c) S. Hammes-Schiffer, A. A. Stuchebrukhov, *Chem. Rev*., 2010, **110**, 6939; d) B. H. Solis, S. Hammes-Schiffer, *Inorg. Chem*., 2011, **50**, 11252; e) L. Hammarströ̈m, S. Styring, *Energy Environ*., 2011, **4**, 2379; f) J. N. Schrauben, M. Cattaneo, T. C. Day, A. L. Tenderholt, J. M. Mayer, *J. Am. Chem. Soc*., 2012, **134**, 16635; g) R. N. Barnett, J. Joseph, U. Landman, G. B. Schuster, *J. Am. Chem. Soc*., 2013, **135**, 3904; h) B. Giese, *Acc. Chem. Res*., 2000, **33**, 631; i) M. Cordes, B. Giese, *Chem. Soc. Rev*., 2009, **38**, 892; j) M. T. Koper, *Phys. Chem.Chem. Phys*., 2013, **15**, 1399.

14 a) C. J. Gagliardi, B. C. Westlake, C. A. Kent, J. J. Paul, J. M. Papanikolas, T. J. Meyer, *Coord. Chem. Rev*., 2010, **254**, 2459; b) N. De Silva, N. Minezawa, M. S. Gordon, *J. Phys. Chem. B*, 2013, **117**, 15386; c) S. Hammes-Schiffer, J. Phys. Chem. Lett., 2011, 2, 1410; d) S. Hammes-Schiffer, *Proc. Natl. Acad. Sci. U.S.A*., 2011, **108**, 8531; e) A. P. Demchenko, K.-C. Tang, P.-T. Chou, *Chem. Soc. Rev*., 2013, **42**, 1379; f) S. M. Aly, A. Usman, M. AlZayer, G. A. Hamdi, E. Alarousu, O. F. Mohammed, *J. Phys. Chem. B*, 2015, **119**, 2596; g) O. F. Mohammed, D. Xiao, V. S. Batista, E. T. J. Nibbering, *J. Phys. Chem. A*, 2014, **118**, 3090; h) D. Shemesh, A. L. Sobolewskib, W. Domcke, *Phys. Chem. Chem. Phys*., 2010, **12**, 4899; i) C. Fang, R. R. Frontiera, R. Tran, R. A. Mathies, *Nature*, 2009, **462**, 200; j) F. Han, W. Liu, C. Fang, *Chem. Phys*., 2013, **422**, 204.

15 a) S. Parmer, R. Kumar, *J. Med. Chem*., 1968, **11**, 635; b) Y. D. Reddy, V. V. Somayajulu, *J. Ind. Chem. Soc*., 1981, **58,** 599; c) Y. Tianzhi, Z. Yuling, F. Duowang, *J. Mol. Struct*., 2006, **791**, 18.

16 a) T. Z. Yu, Y. L. Zhao, X. S. Ding, D. W. Fan, L. Qian, W. K. Dong, *J. Photochem. Photobiol. A*, 2007, **188**, 245; b) D. Ray, P. K. Bharadwaj, *Inorg. Chem*., 2008, **7**, 2252; c) S. R. Trenor, A. R. Shultz, B. J. Love, T. E. *Long, Chem. Rev*., 2004, **104**, 3059; d) Y. Tianzhi, Z. Peng, Z. Yuling, Z. Hui, M. Jing, F. Duowang, *Spectrochim. Acta Part A*, 2009, **73**,168; e) C. Ruikui, Y. Xichuan, T. Haining, S. Licheng, *J. Photochem. Photobiol. A*, 2007, **189**, 295; f) K. D. Singer, S. L. Lalama, J. E. Sohn, R. D. Small, Non-linear optical properties of Organic molecules, Crystals, Academic Press, Orlando, FL, 1987, ch. II-8.

17 L. D. Lavis, R. T. Raines, *ACS Chem. Biol*., 2008, **3**, 142.

18 a) D. E. Polyansky, D. C. Neckers, *J. Phys. Chem. A*, 2005, **109**, 2793; b) R. P. Haugland, M. T. Z. Spence, I. D. Johnson, A. Basey, The Handbook: A Guide to Fluorescent Probes and Labeling Technologies, 10th ed., Molecular Probes, Eugene, OR, 2005; c) So-Y. Park, Y. Kubota, K. Funabiki, M. Matsui, *Chem. Lett*., 2009, **38**, 162.

19 S. Sardari, Y. Mori, K. Horita, R. G. Micetich, S. Nishibe, M. Daneshtalab, *Synthesis Bioorg. Med. Chem*., 1999, **7**, 1933.

20 M. E. Riveiro, A. Moglioni, R. Vazquez, N. Gomez, G. Facorro, L. Piehl, E. R. de Celis, K. Shayo, C. Davio, *Bioorg. Med. Chem*., 2008, **16**, 2665.

21 S. P. Pillai, S. R. Menon, L. A. Mitscher, C. A. Pillai, D. M. Shankel, *J. Nat. Prod*., 1999, **62**, 1358.

22 D. Egan, R. O'kennedy, E. Moran, D. Cox, E. Prosser, D. Thornes, *Drug Metab. Rev*., 1990, **22**, 503.

23 M. Savarese, P. A. Netti, C. Adamo, N. Rega, I. Ciofini, *J. Phys. Chem. B*, 2013, **117**, 16165.

24 I. Adamovic, M. A. Freitag, M. S. Gordon, *J. Chem. Phys*., 2003, **118**, 6725.

25 R. G. Parr, W. Yang, Density-Functional Theory of Atoms, Molecules New York: Oxford University Press. 1989

26 a) K. Kim, K. D. Jordan, *J. Phy. Chem*., 1994, **98(40)**, 10089-10094; b) P. J. Stephens, F. J. Devlin, C. F. Chabalowski, M. J. Frisch, *J. Phy. Chem*.,1994, **98(45)**, 11623; c) W. H. Stevens, H. Basch, M. Krauss, P. Jasien, *Can. J. Chem*., 1992, **70**, 612; d) T. R. Cundari, W. J. Stevens, *J. Chem. Phys*., 1993, **98**, 5555; e) P. J. Hay, W. R. Wadt, *J. Chem. Phys*., 1985, **82**, 270.

27 a) A. D. Becke, *J. Chem. Phys*., 1993, **98**, 5648; b) A. D. Becke, *Phys. ReV. A*, 1998, **38**, 3098; c) C. Lee, W. Yang, and R.G. Parr, *Phys. ReV. B*, 1988, **37**, 785.

28 P. C.Hariharan, J. A. Pople, *Theoret.Chim.Acta*, 1973, **28**, 213.

29 T. H. Dunning, *J. Chem. Phys*., 1989, **90**, 1007.

30 a) A. Dreuw, M. H. Gordon, *Chem. Rev*., 2005, **105**, 4009; b) P. Elliott, F. Furche, K. Burke, *Rev. Comp. Chem*., 2009, **26**, 91; c) S. Hirata, M. H. Gordon, *Chem. Phy. Lett*., 1999, **314**, 291; d) E. Runge, E. K. U. Gross, *Phys. ReV. Lett*., 1984, **52**, 997; e) M. Casida, In Recent Advances in Density Functional Methods: D.P. Chong, Ed., World Scientific: Singapore, 1995; Vol. 1, pp 155; f) R. Bauernschmitt, R. Ahlrichs, *Chem. Phys. Lett*., 1996, **256**, 454; g) R. E. Stratmann, G. E. Scuseria, M. J. Frisch, *J. Chem. Phys*., 1998, **109**, 8218; h) F. Furche, R. Ahlrichs, *J. Chem. Phys*., 2002, **117**, 7433; i) J. Cullen, M. Krykunov, T. Ziegler, *Chem. Phys*., 2011, **391**, 11-18; j) T. Ziegler, M. Krykunov, J. Cullen, *J. Chem. Phys*.,

2012, **136**, 124107; k) A. T. B. Gilbert, N. A. Besley, P. M. W. Gill, *J. Phys. Chem. A*, 2008, **112**, 13164.

31 a) F. Furche, R. Ahlrichs, *J. Chem. Phys*., 2004, **121**, 12772; b) H. Li, C. S. Pomelli, J. H. Jensen, *Theoret.Chim.Acta*, 2003, **109**, 71; c) H. Li, *J.Chem.Phys*., 2009, **131**, 184103; d) Y. Wang, H. Li, *J. Chem. Phys*., 2010, **133**, 034108.

32 T. Yanai, D. P. Tew, N. C. Handy, *Chem.Phys.Lett*., 2004, **393**, 51.

33 A Pedone, *J. Chem. Theory Comput*., 2013, **9**, 4087.

34 NBO 6.0. E. D. Glendening, J. K. Badenhoop, A. E. Reed, J. E. Carpenter, J. A. Bohmann, C. M. Morales, C. R. Landis, F. Weinhold (Theoretical Chemistry Institute, University of Wisconsin, Madison, WI, 2013); http://nbo6.chem.wisc.edu

35 a) M. W. Schmidt, K. K. Baldridge, J. A. Boatz, S. T. Elbert, M. S. Gordon, J. H. Jensen, S. Koseki, N. Matsunaga, K. A. Nguyen, S. J. Su, T. L. Windus, M. Dupuis, J. A. Montgomery, *J. Comp. Chem*., 1993, **14**, 1347; b) M. S. Gordon, M. W. Schmidt, Advances in electronic structure theory: GAMESS a decade later, Chapter 41, pp 1167, in Theory Applications of Computational Chemistry, the first forty years, C. E. Dykstra, G. Frenking, K. S. Kim, G. E. Scuseria, Editors (Elsevier, Amsterdam, 2005).

36 T. Nagata, D. G. Fedorov, T. Sawada, K. Kitaura, M. S. Gordon, *J. Chem. Phys*., 2011, **134**, 034110.

37 M. S. A. Abdel-Mottaleb, B. A. El-sayed, M. M. Abo-Aly, and M. Y. El-Kady, *J. Photochem. Photobiol. A*, 1989, **46**, 379.

38 W. Jivaramonaikul, P Rashatasakhonc and S. Wanichwecharungruang, *Photochem. Photobiol. Sci*., 2010, **9**, 1120.

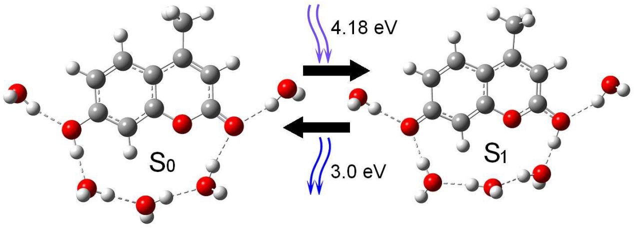

Hydrogen bond dynamics, C-OH bond contracting, O-H bond stretching and O-H···O HB strengthening reveals the ESHT in 4MU at S_1 state.